Hardy-like quantum pigeonhole paradox and the projected-coloring graph state

Weidong Tang *

School of Mathematics and Statistics, Shaanxi Normal University, Xi'an 710119, China

(Received 26 October 2021; revised 22 February 2022; accepted 22 March 2022; published 31 March 2022)

A Hardy-like version of the quantum pigeonhole paradox is proposed, which can also be considered as a special kind of Hardy's paradox. Besides an example induced from the minimal system, a general construction of this paradox from an n-qubit quantum state is also discussed. Moreover, by introducing the projected-coloring graph and the projected-coloring graph state, a pictorial representation of the Hardy-like quantum pigeonhole paradox can be presented. This Hardy-like version of the quantum pigeonhole paradox can be implemented more directly in experiment than the original one, since it does not require some sophisticated techniques such as weak measurements. In addition, from the angle of Hardy's paradox, some Hardy-like quantum pigeonhole paradoxes may be able to set a new record for the success probability of demonstrating Bell nonlocality.

DOI: 10.1103/PhysRevA.105.032457

I. INTRODUCTION

When three two-level quantum particles (qubits) are pre- and postselected in a specific subensemble, an effect of no two particles being in the same quantum state could arise, conflicting with the pigeonhole principle which states that if three pigeons are put into two boxes, necessarily two pigeons will stay in the same box. Such a counterintuitive quantum feature provides an interesting demonstration that quantum correlations cannot be simulated classically, and was referred to as the quantum pigeonhole effect (or paradox) in the seminal work [1] by Aharonov *et al.* In some sense, it can also be regarded as a demonstration of Bell nonlocality [2] or contextuality [3,4] without inequalities.

However, since the quantum pigeonhole paradox is a kind of pre- and postselection [5,6] effect, usually it cannot be implemented directly, and the experimental demonstration requires some sophisticated techniques such as weak measurements [7–9]. To overcome this limitation, a natural thought is to explore new versions of the quantum pigeonhole paradox without pre- and postselection. Following this idea, we find a Hardy-like version of such a paradox [referred to as the "Hardy-like quantum pigeonhole (HLQP) paradox" in what follows], which can also be considered as a special kind of Hardy's paradox [10,11].

On the other hand, although the earliest version of Hardy's paradox [10,11] can be considered as the simplest form of the Bell theorem [12], a major shortcoming is that the success probability of excluding local realistic descriptions of quantum mechanics is not very high (the best record of previous versions is $1/2^{n-1}$ [13], where the qubit number $n \geqslant 3$). This bottleneck may cast a gloom over the application of Hardy's paradox. How to improve that may depend on the investigation of some unconventional Hardy's paradoxes. Since the HLQP paradox is a kind of Hardy's paradox, it may bring some unexpected advantages to address this problem.

In addition, recall that many quantum features can be exhibited vividly by their mathematical counterparts (for example, a kind of multiparticle entanglement can be represented by graphs [14,15]). As far as we know, such elegant counterparts of a Hardy's paradox are very rare (another disadvantage). In order to fill this gap, an exploration for some mathematical counterparts to represent the HLQP paradox is necessary.

In this paper, we present a general construction of the n-qubit HLQP paradox. Besides, in order to give a suitable mathematical counterpart as a representation of the HLQP paradox, we introduce a kind of quantum state called the projected-coloring graph state, which can be represented by a kind of nontraditional graph called a projected-coloring graph. We show that each uncolorable projected-coloring graph can induce a HLQP paradox. Furthermore, we find that some n-qubit HLQP paradoxes (which are also n-qubit Hardy's paradoxes) can provide a greater success probability in showing Bell nonlocality (or contextuality) than previous Hardy's paradoxes ($n > 3$). In the end, we also briefly discuss another kind of quantum paradox called the Hardy-like map coloring paradox, which is essentially equivalent to a specific kind of HLQP paradox.

II. A MINIMAL HARDY-LIKE QUANTUM PIGEONHOLE PARADOX

First, denote by X_i (Y_i, Z_i) the Pauli matrices σ_x (σ_y, σ_z) of the ith qubit and $|0\rangle$ and $|1\rangle$ the two eigenstates (with eigenvalues $+1$ and -1, respectively) of Z. Besides, let two mutually orthogonal states, $|+\rangle = (|0\rangle + |1\rangle)/\sqrt{2}$ and $|-\rangle = (|0\rangle - |1\rangle)/\sqrt{2}$ be two "boxes" and three qubits be three "pigeons." Namely, $X_i = 1$ ($X_i = -1$) indicates that the ith qubit (pigeon) is in the box $|+\rangle$ ($|-\rangle$). Here, $X_i = 1$, for example, denotes the event that X_i is measured and the outcome $+1$ is obtained. To construct a HLQP paradox, one can usually

*wdtang@snnu.edu.cn

assume that the quantum state admits a local hidden variable (LHV) model [2,16] or a noncontextual hidden variable model [3,17,18]. For simplicity, hereinafter we only discuss the HLQP paradox of ruling out the LHV model, and accordingly, we only consider the spacelike separated measurements.

In analogy with the conventional quantum pigeonhole paradox, the minimal system of producing a HLQP paradox also requires three qubits. To begin with, we consider the three-qubit quantum state

$$|\Phi\rangle = \tfrac{1}{2}(|000\rangle - |011\rangle - |101\rangle - |110\rangle). \quad (1)$$

Actually, $|\Phi\rangle$ is a Greenberger-Horne-Zeilinger (GHZ) state [19,20], because $|\Phi\rangle = (|\circlearrowleft\circlearrowleft\circlearrowleft\rangle + |\circlearrowright\circlearrowright\circlearrowright\rangle)/\sqrt{2}$. Here, $|\circlearrowleft\rangle = (|0\rangle + i|1\rangle)/\sqrt{2}$ and $|\circlearrowright\rangle = (|0\rangle - i|1\rangle)/\sqrt{2}$.

Once the qubit i is measured and found in the box $|0\rangle$ in a run of the experiment, the other two qubits ("pigeons"), say, j and k, can be found in the state $|\phi_{ij}^{-}\rangle = \frac{1}{\sqrt{2}}(|0\rangle_i|0\rangle_j - |1\rangle_i|1\rangle_j)$. Namely, if X_j and X_k were assumed to be measured in this run, their values should satisfy $X_jX_k = -1$, which indicates that the qubits j and k cannot stay in the same box. Then one can get the following properties (referred to as "Hardy-like constraints" hereinafter):

$$P(X_2X_3 = -1\,|\,Z_1 = 1) = 1, \quad (2a)$$

$$P(X_1X_3 = -1\,|\,Z_2 = 1) = 1, \quad (2b)$$

$$P(X_1X_2 = -1\,|\,Z_3 = 1) = 1, \quad (2c)$$

$$P(Z_1 = 1,\, Z_2 = 1,\, Z_3 = 1) = \tfrac{1}{4}. \quad (2d)$$

Here, $P(X_2X_3 = -1\,|\,Z_1 = 1)$, for example, is the conditional probability of X_2 and X_3 measured with outcomes satisfying $X_2X_3 = -1$ given that the result of $Z_1 = 1$, and $P(Z_1 = 1, Z_2 = 1, Z_3 = 1)$ stands for the joint probability of obtaining the result of $Z_1 = 1$, $Z_2 = 1$, $Z_3 = 1$. Based on the constraints of Eqs. (2a)–(2c) and Eq. (2d), one can construct a HLQP paradoxical argument as follows.

Consider a run of the experiment for which Z_1, Z_2, and Z_3 are measured and the results $Z_1 = 1$, $Z_2 = 1$, and $Z_3 = 1$ are obtained (it will happen with a probability of 1/4). Assume that the state admits a LHV model. Since we have got $Z_1 = 1$, it follows from Eq. (2a) that if X_2 and X_3 had been measured, their results should satisfy $X_2X_3 = -1$. In fact, from the assumption of locality [21], even if X_1 had been measured on qubit 1, one would still have $X_2X_3 = -1$. Thus in this run the outcomes of measuring X_2 and X_3 (determined by the hidden variables λ) must satisfy $X_2(\lambda)X_3(\lambda) = -1$, indicating that qubits 1 and 2 cannot stay in the same box. Likewise, one can infer that $X_1(\lambda)X_3(\lambda) = -1$ and $X_1(\lambda)X_2(\lambda) = -1$ from the measurement results $Z_2 = 1$ and $Z_3 = 1$, respectively. Therefore any two qubits cannot stay in the same box (for this run), which contradicts with the classical pigeonhole principle (see also Appendix A). Namely, a three-qubit HLQP paradox is produced. As a consequence, one can conclude that quantum correlations cannot be classically simulated and any realistic interpretations of quantum mechanics must be nonlocal.

Besides, it is noted that counterintuitive conclusions of various physical paradoxes usually arise from some improper assumptions. For example, in the conventional quantum pigeonhole paradox, the paradoxical conclusion (a violation of the pigeonhole principle) is achieved by adopting a realistic view of the weak values [1,9,22]. By contrast, in the scenario of the HLQP paradox, this paradoxical conclusion is achieved by using another realistic assumption regarding quantum systems, i.e., the assumption of a LHV model [or more generally, a (non)contextual version of the HLQP paradox can also be achieved by the assumption of noncontextual hidden variable models].

Remark 1. (i) Some quantum state can induce more than one HLQP paradox (e.g., the results of $Z_1 = Z_2 = -1$, $Z_3 = 1$ in the above example can also induce a HLQP paradox, but it is equivalent to the case of replacing $|\Phi\rangle$ with $\frac{1}{2}(|000\rangle + |011\rangle + |101\rangle - |110\rangle)$ and considering the results of $Z_1 = Z_2 = Z_3 = 1$; similar tricks also apply to systems with more qubits). Without loss of generality, hereinafter we only discuss the aforementioned kind of HLQP paradoxes (in which LHV models will be ruled out based on the runs of the experiment that each involved the Pauli-Z observable being measured with the outcome $+1$). (ii) Note that the above three-qubit HLQP paradoxical argument also applies to a more general quantum state $|\Phi'\rangle = \alpha|\Phi\rangle + \beta|111\rangle$, where $|\alpha|^2 + |\beta|^2 = 1$ ($|\alpha| \neq 0$), but essentially this counterintuitive quantum feature arises from the component $|\Phi\rangle$ rather than $|111\rangle$. Thus for simplicity it is enough to show the three-qubit HLQP paradox by resorting to $|\Phi\rangle$. (iii) This three-qubit HLQP paradox can also be regarded as a Hardy's paradox induced from a three-qubit GHZ paradox [19,20].

III. A GENERAL n-qubit ($n \geqslant 3$) HLQP PARADOX

Inspired by the three-qubit HLQP paradox, a general n-qubit HLQP paradox can be constructed based on a special kind of quantum state called the *projected-coloring graph* (PCG) state, and an n-qubit PCG state can usually be defined as

$$|P_n\rangle = \frac{1}{\sqrt{p+1}}\left(|00\cdots0\rangle - \sum_{i\in\mathcal{I}}\theta_i|\vec{0}\rangle_{\bar{\mathcal{S}}_i}|\vec{1}\rangle_{\mathcal{S}_i}\right), \quad (3)$$

where $\mathcal{S}_i \subset \{1, 2, \ldots, n\}$, $2 \leqslant |\mathcal{S}_i| < n$, and $|\mathcal{S}_i \cup \mathcal{S}_j| > \max\{|\mathcal{S}_i|, |\mathcal{S}_j|\}$ ($i \neq j \in \mathcal{I}$); here, $|\mathcal{S}_i|$, for example, denotes the number of qubits in the set $\mathcal{S}_i$. Besides, $|\vec{1}\rangle_{\mathcal{S}_i} \equiv \otimes_{k\in\mathcal{S}_i}|1\rangle_k$ and $|\vec{0}\rangle_{\bar{\mathcal{S}}_i} \equiv \otimes_{k\in\bar{\mathcal{S}}_i}|0\rangle_k$. Moreover, the index set $\mathcal{I}$ is used to describe a group of specific subsets of $\{1, 2, \ldots, n\}$ and the coefficients $\theta_i = \pm1$. Also note that $p = \sum_{i\in\mathcal{I}}|\theta_i|$.

For a given n-qubit PCG state $|P_n\rangle$, one can define a *Hardy matrix A* and its *argumented Hardy matrix B* as follows:

$$A = (A_{ij})_{p\times n}, \quad B = (A|\vec{\Theta}), \quad (4)$$

where the components $A_{ij} = 1$ if $i \in \mathcal{I} = \{1, 2, \ldots, p\}$ and $j \in \mathcal{S}_i$; and $A_{ij} = 0$ otherwise. Besides, the ith component of the vector $\vec{\Theta}$ is $\Theta_i = (\theta_i + |\theta_i|)/2$.

In a run of the experiment, if $Z_{j_1}, Z_{j_2}, \ldots, Z_{j_{n-|\mathcal{S}_i|}}$ ($\{j_1, j_2, \ldots, j_{n-|\mathcal{S}_i|}\} = \bar{\mathcal{S}}_i$) are measured and the results $Z_{j_1} = Z_{j_2} = \cdots = Z_{j_{n-|\mathcal{S}_i|}} = 1$ are obtained, i.e., the qubits in $\bar{\mathcal{S}}_i$ are found in $|\vec{0}\rangle_{\bar{\mathcal{S}}_i}$, then the qubits in $\mathcal{S}_i$ are in the eigenstate of $\prod_{k\in\mathcal{S}_i}X_k$ (with the eigenvalue $-\theta_i$). Therefore, for any $i \in \mathcal{I}$,

$$P\left(\prod_{k\in\mathcal{S}_i}X_k = -\theta_i|Z_{j_1} = Z_{j_2} = \cdots = Z_{j_{n-|\mathcal{S}_i|}} = 1\right) = 1. \quad (5)$$

Besides, denote by $\cup_{i=1}^{p}\bar{\mathcal{S}}_i=\{p_1,p_2,\dots,p_q\}$. Since $|\cup_{i=1}^{p}\bar{\mathcal{S}}_i|>|\bar{\mathcal{S}}_k|$ $(\forall k\in\mathcal{I})$, i.e., the results of obtaining $Z_{p_1}=Z_{p_2}=\cdots=Z_{p_q}=1$ can only arise from the component $|00\cdots0\rangle$ in $|P_n\rangle$, then we can get

$$P(Z_{p_1}=Z_{p_2}=\cdots=Z_{p_q}=1)=\frac{1}{p+1}>0. \tag{6}$$

Note that Eqs. (5) and (6) can provide a total of $p+1$ constraints. Then a practical criterion for constructing the HLQP paradox can be described as follows.

Theorem 1. Given an n-qubit PCG state $|P_n\rangle$, one can always construct a HLQP paradox if $\text{rank}(A)\neq\text{rank}(B)$, where A and B are the corresponding Hardy matrix and argumented Hardy matrix, respectively.

Proof. The proof is similar to the discussion of the aforementioned three-qubit HLQP paradox.

Consider a run of the experiment for which $Z_{p_1},Z_{p_2},\dots,Z_{p_q}$ are measured and the results $Z_{p_1}=1$, $Z_{p_2}=1,\dots,Z_{p_q}=1$ are obtained [it will happen with a probability of $1/(p+1)$ by Eq. (6)], where $\{p_1,p_2,\dots,p_q\}=\cup_{i=1}^{p}\bar{\mathcal{S}}_i$. Assume that $|P_n\rangle$ admits a LHV model. For any $\mathcal{S}_i$ $(1\leqslant i\leqslant p)$, if $Z_{j_1},Z_{j_2},\dots,Z_{j_{n-|\mathcal{S}_i|}}$ and $X_{j_{n-|\mathcal{S}_i|+1}},X_{j_{n-|\mathcal{S}_i|+2}},\dots,X_{j_n}$ were measured in this run (where $\{j_1,j_2,\dots,j_{n-|\mathcal{S}_i|}\}=\bar{\mathcal{S}}_i$, $\{j_n-|\mathcal{S}_i|+1,j_n-|\mathcal{S}_i|+2,\dots,j_n\}=\mathcal{S}_i$), then necessarily $\prod_{k\in\mathcal{S}_i}X_k=-\theta_i$ according to Eq. (5), because in this run $Z_{j_1}=Z_{j_2}=\cdots=Z_{j_{n-|\mathcal{S}_i|}}=1$.

Analogous to the argument of the three-qubit HLQP paradox, as long as the conditions

$$\begin{cases}\prod_{k\in\mathcal{S}_1}X_k=-\theta_1,\\ \prod_{k\in\mathcal{S}_2}X_k=-\theta_2,\\ \vdots\\ \prod_{k\in\mathcal{S}_p}X_k=-\theta_p\end{cases} \tag{7}$$

cannot hold simultaneously (namely, contradict with the pigeonhole principle), a HLQP paradox can be produced. By performing logarithm operations on both sides of each equation (over the complex field), we can get

$$\begin{cases}\sum_{k\in\mathcal{S}_1}\ln X_k=\ln(-\theta_1),\\ \sum_{k\in\mathcal{S}_2}\ln X_k=\ln(-\theta_2),\\ \vdots\\ \sum_{k\in\mathcal{S}_p}\ln X_k=\ln(-\theta_p).\end{cases}$$

Note that the value of each X_k is either $+1$ or -1, and besides, $\ln 1=0$ and $\ln(-1)=\ln(e^{i\pi})=i\pi$. Since $\theta_i=\pm1$, one can get $\ln(-\theta_j)=i\pi(\theta_j+|\theta_j|)/2=i\pi\Theta_j$. Let $y_k=\ln X_k$ be the kth component of vector $\vec{y}$; the above system of equations can be rewritten as

$$A\vec{y}=i\pi\vec{\Theta},$$

where A is the Hardy matrix defined in Eq. (4). This system has at least one solution only if $\text{rank}(A)=\text{rank}(\,A\mid i\pi\vec{\Theta}\,)=\text{rank}(\,A\mid\vec{\Theta}\,)=\text{rank}(B)$. Therefore, if $\text{rank}(A)\neq\text{rank}(B)$, the system of equations (7) has no solution. In this case, a HLQP paradox can be constructed. ■

Note that Theorem 1 can induce a formalized approach to construct a HLQP paradox (which could facilitate the computer search). Based on that, one can even find several analytic constructions for the HLQP paradox. For example, a $(2k+1)$-qubit $(k\geqslant1)$ PCG state with $\mathcal{S}_i=\{i,i+1\}$ $(i=1,2,\dots,2k+1$, and $i+1=1$ if $i=2k+1)$ and $\theta_i=1$, i.e., $|P_{2k+1}\rangle=(|00\cdots0\rangle-|1100\cdots00\rangle-|0110\cdots00\rangle-|0011\cdots00\rangle-\cdots-|0000\cdots11\rangle-|1000\cdots01\rangle)/\sqrt{2k+2}$, can always produce a HLQP paradox, since $\text{rank}(A)=2k$ and $\text{rank}(B)=2k+1$. Obviously, when $k=1$, such a HLQP paradox is exactly the aforementioned three-qubit HLQP paradox. In that case, since $A=\begin{pmatrix}1&1&0\\0&1&1\\1&0&1\end{pmatrix}$ and $B=\begin{pmatrix}1&1&0&1\\0&1&1&1\\1&0&1&1\end{pmatrix}$, one can check that $\text{rank}(A)=2$ and $\text{rank}(B)=3$.

Moreover, note that $\text{rank}(A)\neq\text{rank}(B)$ is only a sufficient condition for constructing a HLQP paradox, since the proof of Theorem 1 is based on a particular choice of the boxes ($|+\rangle$ and $|-\rangle$). However, as long as the boxes are not prescribed, even if $\text{rank}(A)=\text{rank}(B)$ holds, sometimes a HLQP paradox can still be constructed.

For example, consider the state $(|000\rangle+|110\rangle+|101\rangle+|011\rangle)/2$. Namely, $\mathcal{S}_1=\{1,2\}$, $\mathcal{S}_2=\{2,3\}$, and $\mathcal{S}_3=\{1,3\}$, and $\Theta_1=\Theta_2=\Theta_3=0$ $(\theta_1=\theta_2=\theta_3=-1)$. Therefore $A=\begin{pmatrix}1&1&0\\0&1&1\\1&0&1\end{pmatrix}$ and $B=\begin{pmatrix}1&1&0&0\\0&1&1&0\\1&0&1&0\end{pmatrix}$. Then one can get $\text{rank}(A)=\text{rank}(B)$. However, if two boxes are chosen to be $|\circlearrowleft\rangle=(|0\rangle+i|1\rangle)/\sqrt{2}$ and $|\circlearrowright\rangle=(|0\rangle-i|1\rangle)/\sqrt{2}$, a HLQP paradox can still be constructed based on the following constraints:

$$P(Y_2Y_3=-1\,|\,Z_1=1)=1, \tag{8a}$$

$$P(Y_1Y_3=-1\,|\,Z_2=1)=1, \tag{8b}$$

$$P(Y_1Y_2=-1\,|\,Z_3=1)=1, \tag{8c}$$

$$P(Z_1=1,\ Z_2=1,\ Z_3=1)=\tfrac{1}{4}. \tag{8d}$$

In this scenario, one can also present a similar theorem based on such a choice of boxes (by redefining the Hardy matrix A and its augmented matrix B). In fact, this version of the HLQP paradox can be considered as a locally unitary equivalence of the aforementioned three-qubit HLQP paradox. Such kind of equivalence also applies to more complicated cases. Therefore it is enough to discuss the HLQP paradox in one choice of the boxes.

Furthermore, analogous to the statement in point (ii) of Remark 1, one can also construct an n-qubit HLQP paradox from a more general quantum state (see Appendix B for details).

IV. A GRAPHICAL REPRESENTATION OF THE HLQP PARADOX

Many well-known quantum features or phenomena may have some vivid descriptions in terms of their mathematical counterparts, but such elegant descriptions are rare for the Hardy's paradox. To fill the gap, here we shall present a pictorial representation of the HLQP paradox.

To start, let us introduce some notions.

A *projected-coloring graph* $\mathcal{P}=(V,E)$ associated with the PCG state $|P_n\rangle=(|00\cdots0\rangle-\sum_{i\in\mathcal{I}}\theta_i|\vec{0}\rangle_{\bar{\mathcal{S}}_i}|\vec{1}\rangle_{\mathcal{S}_i})/\sqrt{p+1}$ [see Eq. (3)] can be defined as an unconventional weighted graph which consists of a set of vertices $V=\{1,2,\dots,n\}$ and a set of edges $E=\{\mathcal{S}_i|i=1,2,\dots,p\}$ with weights red

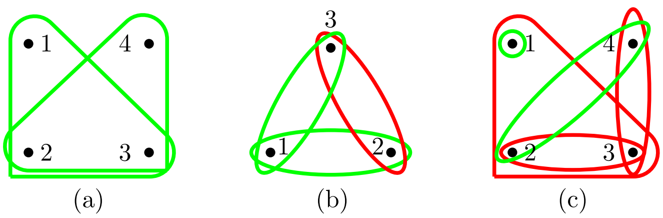

FIG. 1. Simple examples of legal or illegal PCGs, wherein closed green and red curves stand for edges with weights G and R, respectively. (a) The PCG associated with the four-qubit PCG state $|P_4\rangle = (|0000\rangle + |0\rangle_{\{4\}}|\vec{1}\rangle_{\{1,2,3\}} + |0\rangle_{\{1\}}|\vec{1}\rangle_{\{2,3,4\}})/\sqrt{3} = (|0000\rangle + |1110\rangle + |0111\rangle)/\sqrt{3}$, in which two edges are $\mathcal{S}_1 = \{1,2,3\}$ and $\mathcal{S}_2 = \{2,3,4\}$, respectively, and their weights are both G since $\theta_1 = \theta_2 = -1$. (b) The PCG associated with the three-qubit PCG state $|P_3\rangle = (|000\rangle - |0\rangle_{\{1\}}|\vec{1}\rangle_{\{2,3\}} + |0\rangle_{\{2\}}|\vec{1}\rangle_{\{1,3\}} + |0\rangle_{\{3\}}|\vec{1}\rangle_{\{1,2\}})/2 = (|000\rangle - |011\rangle + |101\rangle + |110\rangle)/2$, wherein three edges are $\mathcal{S}_1 = \{1,2\}$, $\mathcal{S}_2 = \{2,3\}$, and $\mathcal{S}_3 = \{1,3\}$, respectively (the weights correlated with $\mathcal{S}_1$, $\mathcal{S}_2$, and $\mathcal{S}_3$ are G, R, and G, respectively). (c) An illegal PCG (the edges are $\mathcal{S}_1 = \{1\}$, $\mathcal{S}_2 = \{1,2,3\}$, $\mathcal{S}_3 = \{2,3\}$, $\mathcal{S}_4 = \{2,4\}$, and $\mathcal{S}_5 = \{2,3\}$; note that $|\mathcal{S}_1 \cup \mathcal{S}_2| = |\{1\} \cup \{1,2,3\}| = 3$ and $|\mathcal{S}_3 \cup \mathcal{S}_2| = |\{2,3\} \cup \{1,2,3\}| = 3$, i.e., the edges $\mathcal{S}_1$ and $\mathcal{S}_3$ are contained in the edge $\mathcal{S}_2$, which obviously does not meet the requirement of a PCG).

(R) and green (G) (corresponding to $\theta_i = 1$ and $\theta_i = -1$, respectively).

According to the definition of $|P_n\rangle$ in Eq. (3), each edge $\mathcal{S}_i$ may connect more than two vertices (here, we use a closed curve circulating two or more vertices to represent an edge), which looks somewhat like an edge of the hypergraph referred to in Ref. [23]. Clearly, such a property is different from that of a conventional graph in which an edge can connect only two vertices. To get a better understanding of that, one can see two simple examples in Figs. 1(a) and 1(b).

Besides, any two edges $\mathcal{S}_i, \mathcal{S}_j \in E$ should satisfy $|\mathcal{S}_i \cup \mathcal{S}_j| > \max\{|\mathcal{S}_i|, |\mathcal{S}_j|\}$ [also see the definition of $|P_n\rangle$ in Eq. (3)]. This will guarantee that each edge cannot be contained in any other edges; see a counterexample in Fig. 1(c).

Moreover, a PCG is called a *connected PCG* if one cannot find a subset $\mathcal{I}' \subset \mathcal{I}$ ($\mathcal{I} = \{1,2,\ldots,p\}$, $0 < |\mathcal{I}'| < |\mathcal{I}|$) such that $(\cup_{i\in\mathcal{I}'}\mathcal{S}_i) \cap (\cup_{j\in(\mathcal{I}-\mathcal{I}')}\mathcal{S}_j) = \emptyset$. Namely, there are no isolated substructures in a connected PCG. For simplicity, hereinafter only connected PCGs are considered.

Next, we consider such a vertex-coloring game: For a given n-vertex PCG $\mathcal{P}$, check whether there exists a consistent coloring scheme for all the vertices, wherein the coloring rules are described as follows.

(i) Each vertex v_k ($v_k \in \{1,2,\ldots,n\}$) can only be colored with either R or G. If v_k is colored by R, its coloring value $c(v_k)$ is defined as $c(v_k) = -1$; otherwise $c(v_k) = 1$.

(ii) If the weight of the edge $\mathcal{S}_i$ is R, its weight value $W(\mathcal{S}_i)$ is defined as $W(\mathcal{S}_i) = -1$; otherwise $W(\mathcal{S}_i) = 1$. Namely, $W(\mathcal{S}_i) = -\theta_i$.

(iii) If there exists at least one vertex-coloring solution, such that $\prod_{v_k\in\mathcal{S}_i} c(v_k) = W(\mathcal{S}_i)$ holds for any $\mathcal{S}_i \in E$, then the PCG $\mathcal{P}$ is colorable; otherwise $\mathcal{P}$ is uncolorable.

Example 1. The PCG is given in Fig. 1(a), and the associated four-qubit PCG state is $|P_4\rangle = (|0000\rangle + |0\rangle_{\{4\}}|\vec{1}\rangle_{\{1,2,3\}} + |0\rangle_{\{1\}}|\vec{1}\rangle_{\{2,3,4\}})/\sqrt{3} = (|0000\rangle + |1110\rangle + |0111\rangle)/\sqrt{3}$, in which four vertices are $v_1 = 1$, $v_2 = 2$, $v_3 = 3$, and $v_4 = 4$ and two edges are $\mathcal{S}_1 = \{1,2,3\}$ and $\mathcal{S}_2 = \{2,3,4\}$. Besides, $\theta_1 = \theta_2 = -1$ [or $W(\mathcal{S}_1) = W(\mathcal{S}_2) = 1$]. Let us consider the vertex coloring of $\mathcal{P}_4$. Note that if this PCG is colorable, $c(1)c(2)c(3) = 1$ and $c(2)c(3)c(4) = 1$ should hold simultaneously, where $c(i) = \pm 1$ for $i = 1,2,3,4$. In fact, there are four solutions that meet this requirement: (i) $c(1) = c(2) = c(3) = c(4) = 1$; (ii) $c(1) = c(4) = 1$, $c(2) = c(3) = -1$; (iii) $c(1) = c(2) = c(4) = -1$, $c(3) = 1$; and (iv) $c(1) = c(3) = c(4) = -1$, $c(2) = 1$. Accordingly, there exist four vertex-coloring solutions for the vertices 1,2,3,4: (G,G,G,G), (G,R,R,G), (R,R,G,R), and (R,G,R,R). Thus this PCG is colorable.

Example 2. Consider the PCG shown in Fig. 2(a). The corresponding PCG state is exactly the state discussed in the aforementioned three-qubit HLQP paradox, i.e., $|\Phi\rangle = (|000\rangle - |0\rangle_{\{3\}}|\vec{1}\rangle_{\{1,2\}} - |0\rangle_{\{2\}}|\vec{1}\rangle_{\{1,3\}} - |0\rangle_{\{1\}}|\vec{1}\rangle_{\{2,3\}})/2 = (|000\rangle - |110\rangle - |101\rangle - |011\rangle)/2$. The three edges are $\mathcal{S}_1 = \{1,2\}$, $\mathcal{S}_2 = \{1,3\}$, and $\mathcal{S}_3 = \{2,3\}$, and their weight values are the same: $W(\mathcal{S}_1) = W(\mathcal{S}_2) = W(\mathcal{S}_3) = -1$ ($\theta_1 = \theta_2 = \theta_3 = 1$). Then if this PCG is colorable, the system of equations $c(1)c(2) = -1$, $c(1)c(3) = -1$, $c(2)c(3) = -1$ should have at least one solution. However, there exist no such consistent solutions. Therefore this PCG is uncolorable. Similar discussions can apply to all the examples shown in Fig. 2.

It is noted that by associating $c(1)$, $c(2)$, and $c(3)$ with the values X_1, X_2, and X_3, respectively, one can connect $c(2)c(3) = -1$, $c(1)c(3) = -1$, $c(1)c(2) = -1$ (in example 2) with a group of inconsistent relations $X_2X_3 = -1$, $X_1X_3 = -1$, $X_1X_2 = -1$. Also note that one can get this group of relations from the Hardy-like constraints given in Eqs. (2a)–(2c), if one consider a run of the experiment that Z_1, Z_2, Z_3 are measured and the results $Z_1 = Z_2 = Z_3 = 1$ are obtained (under the assumption of a LHV model). This indicates that the heart of the paradoxical argument for the aforementioned three-qubit HLQP paradox can be simulated by the uncolorability of this three-vertex PCG, i.e., the PCG shown in Fig. 2(a) can be considered as a pictorial representation of that HLQP paradox. In addition, each edge of the PCG can be connected with a Hardy-like constraint [the edges $\{2,3\}$, $\{1,3\}$, and $\{1,2\}$ of Fig. 2(a) are associated with Eqs. (2a), (2b), and (2c), respectively].

The following theorem will shows us a more general connection between the vertex coloring of a PCG and the HLQP paradox.

Theorem 2. There exists a one-to-one correspondence between an uncolorable PCG and the condition $\text{rank}(A) \neq \text{rank}(B)$, where A and B are the Hardy matrix and argumented Hardy matrix of the corresponding PCG state.

Proof. Notice that in an n-vertex PCG $\mathcal{P}$, the coloring value of the jth ($j \in \{1,2,\ldots,n\}$) vertex $c(j)$ can be associated with the value assigned to X_j of the jth qubit. Besides, the uncolorable condition states that $\prod_{k\in\mathcal{S}_i} c(k) = W(\mathcal{S}_i) = -\theta_i$ ($i \in \mathcal{I}$) cannot hold for all the edges, which corresponds exactly to the system of p equations $\prod_{k\in\mathcal{S}_1} X_k = -\theta_1$, $\prod_{k\in\mathcal{S}_2} X_k = -\theta_2, \ldots, \prod_{k\in\mathcal{S}_p} X_k = -\theta_p$ having no solutions. As mentioned in the proof of Theorem 1, the condition of no solution for this system of equations is equivalent

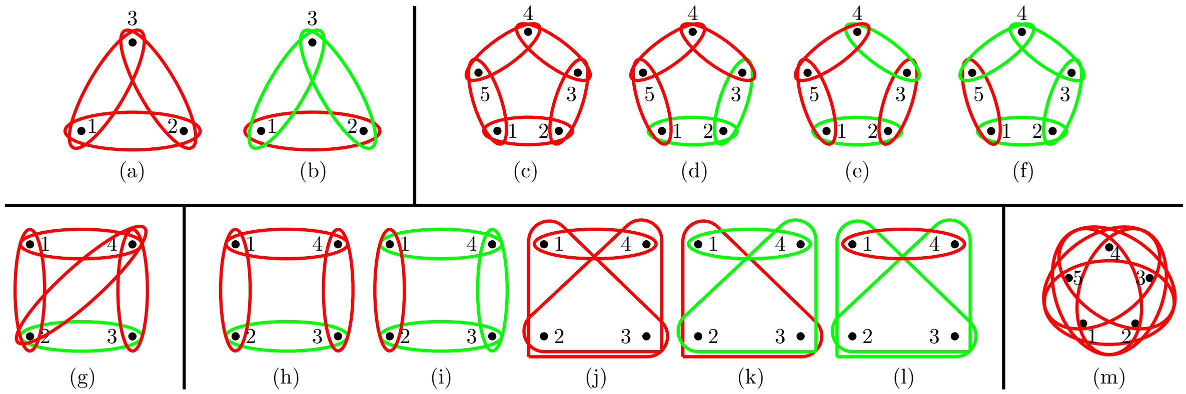

FIG. 2. Examples of uncolorable PCGs. (a)–(f) Some typical three-qubit and five-qubit uncolorable loop PCGs in which each edge contains only two vertices. (g) This PCG contains a three-qubit uncolorable substructure $\mathcal{P}' = (V', E')$, where $V' = \{1, 2, 4\}$ and $E' = \{\{1, 2\}, \{1, 4\}, \{2, 4\}\}$, which implies that it is not an irreducible uncolorable PCG. (h)–(l) Some typical four-qubit uncolorable PCGs. (m) Another five-qubit uncolorable PCG, wherein each edge contains four vertices.

to $\text{rank}(A) \neq \text{rank}(B)$. Then we can get a one-to-one correspondence between an uncolorable PCG and the condition $\text{rank}(A) \neq \text{rank}(B)$. ■

On the other hand, one can check that an n-vertex colorable PCG will give rise to $\text{rank}(A) = \text{rank}(B)$.

Besides, the above proof also implies another general one-to-one correspondence, i.e., for any Hardy-like constraints given in terms of Eq. (5) [rather than Eq. (6)], there exists an edge in the PCG associated with it, and vice versa. Since such a correspondence for Fig. 2(a) has been discussed above, here we give another more complicated example.

Example 3. The PCG in Fig. 2(d) is associated with the PCG state $(|00000\rangle + |11000\rangle + |01100\rangle - |00110\rangle - |00011\rangle - |10001\rangle)/\sqrt{6}$. $\mathcal{S}_1 = \{1, 2\}$, $\mathcal{S}_2 = \{2, 3\}$, $\mathcal{S}_3 = \{3, 4\}$, $\mathcal{S}_4 = \{4, 5\}$, and $\mathcal{S}_5 = \{1, 5\}$ are five edges with weights G, G, R, R, and R [or their weight values are $W(\mathcal{S}_1) = 1$, $W(\mathcal{S}_2) = 1$, $W(\mathcal{S}_3) = -1$, $W(\mathcal{S}_4) = -1$, and $W(\mathcal{S}_5) = -1$], respectively. One can easily check that there are no consistent solutions for $c(1)c(2) = 1$, $c(2)c(3) = 1$, $c(3)c(4) = -1$, $c(4)c(5) = -1$, $c(1)c(5) = -1$, indicating that this PCG is uncolorable. As mentioned in the proof of Theorem 2, one can define a one-to-one connection between the system of equations $c(1)c(2) = 1$, $c(2)c(3) = 1$, $c(3)c(4) = -1$, $c(4)c(5) = -1$, $c(1)c(5) = -1$ and the system $X_1X_2 = 1$, $X_2X_3 = 1$, $X_3X_4 = -1$, $X_4X_5 = -1$, $X_1X_5 = -1$. The former is induced from the edges $\mathcal{S}_1 = \{1, 2\}$, $\mathcal{S}_2 = \{2, 3\}$, $\mathcal{S}_3 = \{3, 4\}$, $\mathcal{S}_4 = \{4, 5\}$, and $\mathcal{S}_5 = \{1, 5\}$, while the latter is induced from the Hardy-like constraints $P(X_1X_2 = 1 \,|\, Z_3 = Z_4 = Z_5 = 1) = 1$, $P(X_2X_3 = 1 \,|\, Z_1 = Z_4 = Z_5 = 1) = 1$, $P(X_3X_4 = -1 \,|\, Z_1 = Z_2 = Z_5 = 1) = 1$, $P(X_4X_5 = -1 \,|\, Z_1 = Z_2 = Z_3 = 1) = 1$, and $P(X_1X_5 = -1 \,|\, Z_2 = Z_3 = Z_4 = 1) = 1$. From this angle, these Hardy-like constraints can be represented by the edges of the PCG.

Furthermore, according to Theorem 1, for an n-qubit PCG state $|P_n\rangle$, if $\text{rank}(A) \neq \text{rank}(B)$, a HLQP paradox can be constructed, and from Theorem 2, one can see that the corresponding PCG $\mathcal{P}$ is uncolorable. Thus the HLQP paradox induced from a PCG state can be represented by an uncolorable PCG.

Next, an n-qubit HLQP paradox is said to be a *genuinely n-qubit HLQP paradox* if one cannot reduce the number of Hardy-like constraints and still have a HLQP paradox. Besides, the corresponding PCG is called an *irreducible uncolorable PCG*.

Notice that each edge of an uncolorable PCG is associated with a Hardy-like constraint of the correlated HLQP paradox. Then another definition of the irreducible uncolorable PCG can be described as follows: For a given uncolorable PCG, it would become colorable if any edge is deleted, and then such an uncolorable PCG is irreducible. In other words, an irreducible uncolorable PCG has no uncolorable substructures. Clearly, Figs. 2(a)–2(f) and 2(h)–2(m) are all irreducible uncolorable PCGs. This is because if any of their edges are deleted, they would no longer be uncolorable PCGs. In contrast, Fig. 2(g) is not an irreducible PCG, as it has an uncolorable substructure.

Since an n-vertex irreducible uncolorable PCG is correlated to a genuinely n-qubit HLQP paradox, it is very helpful in the study of the optimization of a HLQP paradox.

Remark 2. (i) Uncolorable PCGs are also very useful in the study of the conventional quantum pigeonhole paradox (see Appendix C). (ii) Unlike the graph (or hypergraph) state [14,15,23], the PCG state is a "conditional subsystem stabilizer state" rather than a stabilizer state, and sometimes this may bring us some unexpected advantages.

V. THE SUCCESS PROBABILITY OF RULING OUT LHV THEORIES

For an n-qubit Hardy's paradox, the maximal success probability of excluding local realism in previous versions [13,24] is $1/2^{n-1}$. Actually, this probability can be greatly improved by some HLQP paradoxes. For example, consider the HLQP paradox induced from the PCG state (associated with an n-vertex loop PCG) $|A_{L_n}\rangle = \frac{1}{\sqrt{n+1}}(|\vec{0}\rangle_V - |1\rangle_1|1\rangle_n|\vec{0}\rangle_{V\setminus\{1,n\}} + \sum_{i=1}^{n-1}|1\rangle_i|1\rangle_{i+1}|\vec{0}\rangle_{V\setminus\{i,i+1\}})$. Clearly, the success probability is $P_n^L = 1/(n+1)$, which decays much slower over n than P_n^G and P_n^S listed in Table I. Namely, this HLQP paradox is

TABLE I. The success probabilities of three kinds of Hardy's paradoxes for n qubits.

Scenario	Success probability ($n \geqslant 3$)[a]
Loop PCG state induced	$P_n^L = 1/(n+1)$
Generalized, Ref. [13]	$P_n^G = 1/2^{n-1}$
Standard, Ref. [24]	$P_n^S = 1/2^n \times (1 + \cos \frac{\pi}{n-1})$

[a]For $n \geqslant 3$, $P_n^L \geqslant P_n^G > P_n^S$.

more efficient [25] in demonstrating Bell nonlocality than two representative Hardy's paradoxes [13,24].

VI. HARDY-LIKE MAP COLORING PARADOX

Besides the uncolorable PCGs, other mathematical objects or problems that mimic some specific HLQP paradoxes can also be found, such as the map coloring problem, in which for a given planar map, usually four colors are required to guarantee that no two adjacent regions have the same color (also known as the four-color theorem [26]). In other words, using two or three colors to color the planar map, one cannot ensure each pair of adjacent regions to have different colors in most situations. Here, a simple example based on the map coloring problem will be presented, and it will be referred to as the "Hardy-like map coloring paradox."

To construct a Hardy-like quantum map coloring paradox, we associate a quantum state with a map (each region stands for a qubit) and use the value (± 1) of X_i of the ith qubit in a run of the experiment to label the "color" of the ith region, i.e., only two colors are involved in such a map. One can infer that for a great number of such maps, one can always find two adjacent regions sharing the same color according to the four-color theorem stated above.

As an example, we associate $|M(4)\rangle = \frac{1}{\sqrt{7}}(|0000\rangle - |1100\rangle - |1010\rangle - |1001\rangle - |0110\rangle - |0101\rangle - |0011\rangle)$ with the map of Fig. 3(a). Assume that $|M(4)\rangle$ can be modeled by LHV; then a paradoxical conclusion can be produced as follows. Consider a run of the experiment for which Z_1, Z_2, Z_3, Z_4 are measured and the results $Z_1 = Z_2 = Z_3 = Z_4 = 1$ are obtained (this would happen with a probability of $1/7$). Since we have $Z_a = Z_b = 1$ ($a \neq b \in \{1, 2, 3, 4\}$), then according to the assumption of local realism, if X_c and X_d ($c \neq d \neq a \neq b \in \{1, 2, 3, 4\}$) had been measured in this run, their results should satisfy $X_d X_d = -1$. As a consequence, if X_1, X_2, X_3, X_4 were measured in this run, one can infer that $X_1X_2 = X_1X_3 = X_1X_4 = X_2X_3 = X_2X_4 = X_3X_4 = -1$, which indicates that no two adjacent regions have the same color.

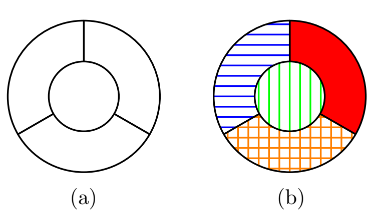

FIG. 3. (a) A map to be colored by two colors. (b) At least four colors are required to guarantee that no two adjacent regions have the same color for this map.

Clearly, to achieve that, at least four colors are required; see the illustration in Fig. 3(b). However, only two colors are used in this map, which implies that there should have been some adjacent regions sharing the same color, a contradiction. Then one can get a Hardy-like quantum map coloring paradox.

Similar constructions can also apply to a great number of planar maps called *bicolor uncolorable maps* (for which there exist no consistent coloring solutions, if two adjacent regions sharing the same color is forbidden and only two colors are provided). Clearly, the Hardy-like map coloring paradox is another manifestation of a HLQP paradox, and the bicolor uncolorable map can be regarded as the representation for this quantum paradox.

In contrast with the uncolorable PCG representation, it seems more intuitive to understand some specific HLQP paradoxes from the angle of map coloring problems, since these problems are based on many people's common sense (four-color theorem) and in many situations one does not really have to check all possible colorings (the contradiction is too obvious). However, the shortcoming is that the bicolor uncolorable map representation can only be considered as a subclass of the uncolorable PCG representation (it only applies to the planar graphical structure and cannot describe a PCG with edges containing more than two vertices).

VII. DISCUSSION AND CONCLUSION

To summarize, we have studied the general construction of the n-qubit Hardy-like quantum pigeonhole (HLQP) paradox (which is also a special class of Hardy's paradox). In addition, by introducing the notions of the PCG state and the PCG, we give a pictorial representation of the HLQP paradox. This paradox has several advantages. From the angle of the quantum pigeonhole paradox, the HLQP paradox scheme seems to be more friendly to the experimental physicist, and from the perspective of Hardy's paradox, a family of HLQP paradoxes has surpassed $[1/(n+1)]$ previously reported values for the success probability of demonstrating Bell nonlocality (the record of the previous Hardy's paradoxes is $1/2^{n-1}$; see Ref. [13]).

Some extended topics require further investigation, such as the qudit PCG state, the qudit HLQP paradox, and the analytic construction of some HLQP paradoxes. On the other hand, notice that any stabilizer of a system can exhibit a kind of symmetry. However, usually a PCG state is only a "conditional subsystem stabilizer state" rather than a full-system stabilizer state. The breaking of such a stabilizer symmetry may lead to some unknown properties and unexpected advantages. For example, "all-versus-nothing" proofs [27] of Bell nonlocality which work for 100% of the runs of the experiments (e.g., the GHZ paradox) are commonly induced from perfect correlations [19,28] of the quantum states. However, so far, such proofs induced from systems with nonperfect correlations are still very rare. By noticing that PCG states may induce more than one HLQP paradox [see point (i) of Remark 1] and combining them together might give a stronger demonstration of Bell nonlocality [29], one could construct such all-versus-nothing proofs from some PCG states with nonperfect correlations [30], which may have some potential applications in quantum information protection.

In addition, since every property of quantum mechanics not present in classical physics could lead to an operational advantage [31–33], we believe that the HLQP paradox can also provide us some useful resources in certain quantum information processing.

ACKNOWLEDGMENTS

We thank S. Ru, S. Paraoanu, F. Li, and N. Liu for useful suggestions and discussions. In addition, we would like to thank an anonymous referee for constructive comments and suggestions.

APPENDIX A: ANOTHER WAY TO GET THE CONTRADICTION OF THE THREE-QUBIT HLQP PARADOX

If $|\Psi\rangle$ admits a LHV model, then Eqs. (2a)–(2c) in the main text imply that $\{Z_1 = 1\} \subset \{X_2X_3 = -1\}$, $\{Z_2 = 1\} \subset \{X_1X_3 = -1\}$, and $\{Z_3 = 1\} \subset \{X_1X_2 = -1\}$. One can get $P(Z_1 = 1, Z_2 = 1, Z_3 = 1) \leqslant P(X_2X_3 = -1, X_1X_3 = -1, X_1X_2 = -1) = 0$, which contradicts with Eq. (2d).

APPENDIX B: A MORE GENERAL FORM OF THE QUANTUM STATE THAT CAN INDUCE AN *n*-QUBIT HLQP PARADOX

As mentioned in Remark 1 of the main text, the three-qubit HLQP paradox can also be induced from a more general quantum system $|\Phi'\rangle = \alpha|\Phi\rangle + \beta|111\rangle$, where $|\alpha|^2 + |\beta|^2 = 1$ $(|\alpha| \neq 0)$. It is noted that the term $|111\rangle$ does not cause any essential changes in the demonstration of the three-qubit HLQP paradox.

Likewise, if an n-qubit HLQP paradox can be induced from the state $|P_n\rangle$ [see Eq. (3) of the main text], then such a HLQP paradox can also be induced from a more general quantum system

$$|P_n'\rangle = \alpha|P_n\rangle + \beta|B_n\rangle, \tag{B1}$$

where $|\alpha|^2 + |\beta|^2 = 1$ $(|\alpha| \neq 0)$, $\langle P_n|B_n\rangle = 0$, and

$$|B_n\rangle = \sum_{i\in\mathcal{J}} \lambda_i|\vec{0}\rangle_{\bar{\mathcal{T}}_i}|\vec{1}\rangle_{\mathcal{T}_i}. \tag{B2}$$

Here, $\mathcal{T}_i \subset \{1, 2, \dots, n\}$ and $|\bar{\mathcal{S}}_r \cap \bar{\mathcal{T}}_s| < |\bar{\mathcal{S}}_r|$ $(\forall r, s)$, wherein $\bar{\mathcal{S}}_r$ has been defined in Eq. (3) of the main text. Besides, the index set $\mathcal{J}$ is used for describing all possible $\mathcal{T}_i$ and the coefficient $\lambda_i \in \mathcal{C}$.

Similarly, the term $|B_n\rangle$ does not cause any essential changes in the demonstration of the n-qubit HLQP paradox. In fact, here the component $|B_n\rangle$ can be considered as a generalization of the term $|111\rangle$ in $|\Phi'\rangle$.

APPENDIX C: ANOTHER TYPE OF CONVENTIONAL QUANTUM PIGEONHOLE PARADOX FOR THREE QUBITS

Sometimes uncolorable PCGs are helpful in looking for new conventional quantum pigeonhole paradoxes. For example, Fig. 2(b) in the main text can induce another type of quantum pigeonhole paradox, while Fig. 2(a) corresponds to the original quantum pigeonhole paradox [1].

The initial state is prepared in $|\Phi_i\rangle = |+\rangle|-\rangle|+\rangle$, and the final state is $|\Phi_f\rangle = |0\rangle|1\rangle|0\rangle$. Here, two boxes are $|\circlearrowleft\rangle = (|0\rangle + i|1\rangle)/\sqrt{2}$ and $|\circlearrowright\rangle = (|0\rangle - i|1\rangle)/\sqrt{2}$. One can find $\langle\Phi_i|\frac{I+Y_1Y_2}{2}|\Phi_f\rangle = \langle\Phi_i|\frac{I-Y_1Y_3}{2}|\Phi_f\rangle = \langle\Phi_i|\frac{I-Y_2Y_3}{2}|\Phi_f\rangle = 0$. Therefore, at intermediate times if the qubits $\{1, 3\}$ were measured, they would be found in the same box, and likewise, if the qubits $\{2, 3\}$ were measured, they would also be found in the same box. However, if the qubits $\{1, 2\}$ were measured, the case would be different, i.e., they would be found in different boxes, a contradiction according to the classical pigeonhole principle.

[1] Y. Aharonov, F. Colombo, S. Popescu, I. Sabadini, D. C. Struppa, and J. Tollaksen, Quantum violation of the pigeonhole principle and the nature of quantum correlations, Proc. Natl. Acad. Sci. USA **113**, 532 (2016).

[2] J. S. Bell, On the Einstein Podolsky Rosen paradox, Phys. Phys. Fiz. **1**, 195 (1964).

[3] S. Kochen and E. P. Specker, The problem of hidden variables in quantum mechanics, in *The Logico-algebraic Approach to Quantum Mechanics* (Springer, New York, 1975), pp. 293–328.

[4] S. Yu and C. H. Oh, Quantum pigeonhole effect, Cheshire cat and contextuality, arXiv:1408.2477.

[5] Y. Aharonov, P. G. Bergmann, and J. L. Lebowitz, Time Symmetry in the Quantum Process of Measurement, Phys. Rev. **134**, B1410 (1964).

[6] M. S. Leifer and R. W. Spekkens, Pre- and Post-Selection Paradoxes and Contextuality in Quantum Mechanics, Phys. Rev. Lett. **95**, 200405 (2005).

[7] Y. Aharonov, D. Z. Albert, and L. Vaidman, How the Result of a Measurement of a Component of the Spin of a Spin-1/2 Particle can Turn Out to be 100, Phys. Rev. Lett. **60**, 1351 (1988).

[8] M. Waegell, T. Denkmayr, H. Geppert, D. Ebner, T. Jenke, Y. Hasegawa, S. Sponar, J. Dressel, and J. Tollaksen, Confined contextuality in neutron interferometry: Observing the quantum pigeonhole effect, Phys. Rev. A **96**, 052131 (2017).

[9] M.-C. Chen, C. Liu, Y.-H. Luo, H.-L. Huang, B.-Y. Wang, X.-L. Wang, L. Li, N.-L. Liu, C.-Y. Lu, and J.-W. Pan, Experimental demonstration of quantum pigeonhole paradox, Proc. Natl. Acad. Sci. USA **116**, 1549 (2019).

[10] L. Hardy, Quantum Mechanics, Local Realistic Theories, and Lorentz-Invariant Realistic Theories, Phys. Rev. Lett. **68**, 2981 (1992).

[11] L. Hardy, Nonlocality for Two Particles without Inequalities for Almost All Entangled States, Phys. Rev. Lett. **71**, 1665 (1993).

[12] N. D. Mermin, Quantum mysteries refined, Am. J. Phys. **62**, 880 (1994).

[13] S.-H. Jiang, Z.-P. Xu, H.-Y. Su, A. K. Pati, and J.-L. Chen, Generalized Hardy's Paradox, Phys. Rev. Lett. **120**, 050403 (2018).

[14] R. Raussendorf and H. J. Briegel, A One-Way Quantum Computer, Phys. Rev. Lett. **86**, 5188 (2001).

[15] M. Hein, J. Eisert, and H. J. Briegel, Multiparty entanglement in graph states, Phys. Rev. A **69**, 062311 (2004).

[16] J. F. Clauser, M. A. Horne, A. Shimony, and R. A. Holt, Proposed Experiment to Test Local Hidden-Variable Theories, Phys. Rev. Lett. **23**, 880 (1969).

[17] J. S. Bell, On the problem of hidden variables in quantum mechanics, Rev. Mod. Phys. **38**, 447 (1966).

[18] N. D. Mermin, Hidden variables and the two theorems of John Bell, Rev. Mod. Phys. **65**, 803 (1993).

[19] D. M. Greenberger, M. A. Horne, and A. Zeilinger, Going beyond Bell's theorem, in *Bell's Theorem, Quantum Theory and Conceptions of the Universe* (Springer, New York, 1989), pp. 69–72.

[20] D. M. Greenberger, M. A. Horne, A. Shimony, and A. Zeilinger, Bell's theorem without inequalities, Am. J. Phys. **58**, 1131 (1990).

[21] A. Einstein, B. Podolsky, and N. Rosen, Can Quantum-Mechanical Description of Physical Reality Be Considered Complete? Phys. Rev. **47**, 777 (1935).

[22] R. Corrêa and P. L. Saldanha, Apparent quantum paradoxes as simple interference: Quantum violation of the pigeonhole principle and exchange of properties between quantum particles, Phys. Rev. A **104**, 012212 (2021).

[23] M. Gachechiladze, C. Budroni, and O. Gühne, Extreme Violation of Local Realism in Quantum Hypergraph States, Phys. Rev. Lett. **116**, 070401 (2016).

[24] J. L. Cereceda, Hardy's nonlocality for generalized *n*-particle GHZ states, Phys. Lett. A **327**, 433 (2004).

[25] Note that there also exist HLQP paradoxes which can seemingly provide a greater success probability than P_n^L, for example, the HLQP paradox induced from $\frac{1}{2}(|\vec{0}\rangle_V - |1\rangle_1|1\rangle_2|\vec{0}\rangle_{V\setminus\{1,2\}} - |1\rangle_1|\vec{0}\rangle_{V\setminus\{1\}} - |1\rangle_2|\vec{0}\rangle_{V\setminus\{2\}})$. The success probability is $P_n^T = 1/4$ (constant). However, this class of the HLQP paradox can be proven to be equivalent to a three-qubit HLQP paradox.

[26] F. P. Miller, A. F. Vandome, and J. Mcbrewster, *Four Color Theorem* (Alphascript, Houston, TX, 2010).

[27] N. D. Mermin, Extreme Quantum Entanglement in a Superposition of Macroscopically Distinct States, Phys. Rev. Lett. **65**, 1838 (1990).

[28] A. Cabello, O. Gühne, and D. Rodríguez, Mermin inequalities for perfect correlations, Phys. Rev. A **77**, 062106 (2008).

[29] A. Cabello, Bell's Theorem without Inequalities and without Probabilities for Two Observers, Phys. Rev. Lett. **86**, 1911 (2001).

[30] W. Tang, Perfect demonstration of Bell nonlocality without inequalities from non-perfect correlations, arXiv:2201.01886.

[31] J. M. Matera, D. Egloff, N. Killoran, and M. B. Plenio, Coherent control of quantum systems as a resource theory, Quantum Sci. Technol. **1**, 01LT01 (2016).

[32] M. Hillery, Coherence as a resource in decision problems: The Deutsch-Jozsa algorithm and a variation, Phys. Rev. A **93**, 012111 (2016).

[33] T. Theurer, N. Killoran, D. Egloff, and M. B. Plenio, Resource Theory of Superposition, Phys. Rev. Lett. **119**, 230401 (2017).